

Response to Referee #1 Comments

General Comment:

The Normalized Difference Snow Index (NDSI) is vital in snow cover extent, snow cover fraction, and snow depth retrieving in case of using optical satellite observations. In this study, the authors developed an integrated cloud-free MODIS NDSI over China with the help of a spatio-temporal Adaptive fusion method. However, the following global and regional cloud-free gap-filled NDSI and snow cover extent dataset are excluded in this study, neither in the introduction section, nor in the cross-comparison section. Therefore, it is difficult for me to evaluate whether this dataset is uniqueness or usefulness.

The existing cloud-free NDSI dataset and snow cover extent datasets including:

- MODIS/Terra CGF Snow Cover Daily L3 Global 500m SIN Grid, Version 61 (<https://doi.org/10.5067/MODIS/MOD10A1F.061>), which provide a cloud-gap-filled daily MODIS NDSI dataset at 500m spatial resolution.
- The NIEER AVHRR snow cover extent product over China (<https://essd.copernicus.org/articles/13/4711/2021/>, <https://doi.org/10.5194/essd-13-4711-2021>), which provide a cloud-gap-filled daily AVHRR snow cover extent dataset over China.
- The daily MODIS 500m snow cover extent over China (<http://data.casnw.net/portal/metadata/be3a4134-2e5c-467f-8a5e-b1c0ed6cc341>, doi:10.12072/ncdc.I-SNOW.db0001.2020)
- Daily fractional snow cover dataset over High Asia during 2002 to 2018 (<http://www.ncdc.ac.cn/portal/metadata/0e277d66-d89b-4e54-8a75-fe22fcc3adee>, doi:10.11922/sciencedb.457)

Although the study may content material worthy of publication, the paper in its current version needs major revision and resubmission to meet the level expected of ESSD, for the following reasons.

General Response:

Thank you very much for the critical comments and suggestions regarding our article. Considering all the constructive comments, we carefully revised the Introduction and supplemented the cross-comparison experiments. We searched various existing cloud-free snow cover products covering China and added descriptions in the Introduction. Moreover, to elaborate the reliability of our STAR NDSI collection, we performed comparative experiments between **four existing snow cover products** and ours, all of which revealed the superiority of our

collection. **All quantitative evaluation results are presented in Appendix A of the response.** However, due to space limitations, we only added cross-comparisons with two typical datasets (NIEER AVHRR SCE and MODIS CGF NDSI products, considering spatial coverage and unrestricted access of datasets) in the manuscript.

In summary, the main points of the revisions include: (1) Typical long-term cloud-free snow cover products covering most snow-dominated regions in China were described in Introduction and listed in Table 1 (Section 1). (2) The classification accuracy of STAR NDSI collection was compared with those of TAC NDSI and NIEER AVHRR SCE datasets based on in-situ snow depth measurements (Section 3.1). (3) The numerical accuracy of STAR NDSI collection was compared with those of TAC NDSI and MODIS CGF NDSI datasets based on Landsat NDSI maps (Section 3.2).

Q1. Literature review in Introduction disregards former studies on NDSI retrievals from satellite data, including both datasets retrieval methods. Thus, the contribution of the current study in accordance to existing knowledge and methods is not clear. Please add the above listed cloud-free NDSI dataset and snow cover extent datasets in the introduction section.

Response: Thank you for the comment. We added the descriptions of various existing cloud-free snow cover products in the Introduction as follows:

...On the national scale, Huang et al. (2016) obtained a long-term cloud-removed SCA product using a multi-source data fusion method. Despite many relevant studies, only a few cloud-free snow cover datasets have been released publicly.

Several typical long-term cloud-free snow cover products available online are listed in Table 1 (datasets are referenced via DOI), which cover most snow-dominated regions in China. Huang provided MODIS daily cloudless SCA products with relatively accurate snow detection capabilities in Northern Hemisphere based on multi-source data. Muhammad and Thapa (2021) obtained a daily MODIS SCA and glacier composite dataset for High Mountain Asia by aggregating seasonal, temporal, and spatial filters, which can serve as a valuable input for hydrological and glaciological investigations. Hao et al. (2021) yielded two long-term daily SCA datasets over China through a series of processes such as quality control, cloud detection, snow discrimination, and gap-filling (including hidden Markov random field and snow-depth interpolation techniques). Their releases and updates promoted the research of snow cover characteristics in China. Qiu et al. yielded a daily FSC dataset with detailed snow cover information over High Mountain Asia with MDC and spatial filtering. Additionally, the global cloud-gap-filled MODIS NDSI dataset (MOD10A1F) is available online since 2020, where cloud-covered grids in the MODIS Terra NDSI product are filled by retaining clear-sky observations from previous days (Hall and Riggs, 2020). However, this dataset

performs poorly in China, where periodic and transient snow is dominant. In general, cloud-free SCA datasets produced by composite algorithms are frequently released, while high-quality cloud-free NDSI datasets are still scarce.

To this end, this study generates a spatiotemporally continuous NDSI product with satisfactory accuracy for China, fully considering the spatio-temporal characteristics of regional snow cover variability. A Spatio-Temporal Adaptive fusion method with error correction (STAR) improved from our previous work (Jing et al., 2019) is utilized to eliminate cloud obscuration...

Table 1. Typical long-term cloud-free snow cover products covering most snow-dominated regions in China.

References	Type	Spatial coverage	Temporal coverage	Temporal resolution	Spatial resolution	DOI
Hao et al. (2020)	SCA	China	2000–2020	Daily	~500 m	10.12072/ncdc.I-SNOW.db0001.2020
Hao et al. (2021)	SCA	China	1981–2019	Daily	~5 km	10.11888/Snow.tpd.271381
Huang (2020)	SCA	Northern hemisphere	2000–2015	Daily	~1 km	10.12072/ncdc.CCI.db0044.2020
Muhammad and Thapa (2021)	SCA	High Mountain Asia	2002–2019	Daily	~500 m	10.1594/PANGAEA.918198
Qiu et al. (2017)*	FSC	High Mountain Asia	2002–2018	Daily	~500 m	10.11922/sciencedb.457
Hall and Riggs (2020)	NDSI	Global coverage	2000–present	Daily	~500 m	10.5067/MODIS/MOD10A1F.061

*Cloud coverage is less than 10%.

Q2. The lack of innovation in accordance to existing knowledge. Please add the comparison between NDSI dataset in present study and MODIS/Terra CGF Snow Cover Daily L3 Global 500m SIN Grid, Version 61, both in fusion method and results.

Response: Thank you for the critical comment. The innovations of this work can be summarized as follows:

For the methodology, the clouds in original snow cover products are generally removed by a multi-step combination method. An accumulated cloud-free result can be obtained by combining the spatial methods and temporal methods alternately. However, the independent and successive utilization cannot take full consideration of the spatio-temporal information. Therefore, STAR NDSI collection is generated by a novel Spatio-Temporal Adaptive fusion method with error correction (STAR), which consists of space partition, adaptive space-time block determination, Gaussian kernel function-based fusion, and error correction. This method comprehensively considers spatial and temporal contextual information and thus is promising for the cloud removal of NDSI products.

From a product perspective, cloud-free SCA datasets produced by composite algorithms are frequently released, while high-quality cloud-free NDSI datasets are still scarce. NDSI datasets can provide detailed characteristics of snow cover, which can effectively reduce the confusion of mixed pixels in SCA products. Therefore, the release of cloud-free NDSI datasets with high accuracy is of great significance.

In addition, to elaborate the accuracy of our STAR NDSI collection, **we added two cross-comparisons with two typical snow cover datasets** including NIEER AVHRR SCE (Hao et al., 2021) and MODIS CGF NDSI (Hall and Riggs, 2020) products. The main revisions are as follows:

3 Results

As mentioned above, the generation procedure of continuous snow collection includes the pre-process TAC and the key-process STAR. The remainder clouds of 30.62% in the entire collection after TAC are completely removed by STAR. To elaborate the reliability of STAR NDSI collection, TAC NDSI, NIEER AVHRR SCE, and MODIS CGF NDSI products are used as baseline data. Specifically, based on in-situ snow depth measurements, the classification accuracy of STAR NDSI collection is compared with those of TAC NDSI and NIEER AVHRR SCE datasets. In addition, based on Landsat NDSI maps, its numerical accuracy is compared with those of TAC NDSI and MODIS CGF NDSI datasets. This section presents the evaluation results, followed by an exemplary application.

3.1 Validation against in-situ snow depth measurements

As described above, the in-situ snow depth data in XJ from 1 January 2001 to 31 August 2007 and on TP from 1 August 2000 to 31 December 2013, were used as the ground truth to evaluate the classification accuracy of TAC NDSI, NIEER AVHRR SCE, and STAR NDSI datasets. The nearest pixel was matched with each meteorological station, with a total of about 600000 data pairs. Snow-clad pixels in NDSI datasets range from 10 to 100, whereas snow-free pixels are 0; thus, the classification threshold is set as 10 (Zhang et al., 2019). The discriminant threshold for in-situ snow depth is set as 0 or 1 cm. In addition, the cloud-covered areas in TAC NDSI dataset are considered to be snow-free.

Table 4 demonstrates that NIEER AVHRR SCE and STAR NDSI datasets preeminently capture the snow dynamics in XJ referring to the in-situ measurements, with OAs more than 90%. However, TAC NDSI dataset is insufficient to accurately describe the snow cover variability. Although CEs perform well regardless of the snow depth threshold, OEs of TAC NDSI collection are extremely high, indicating that many cloud-covered areas are dominated by snow. NIEER AVHRR SCE dataset partially retrieves snow pixel under cloud obstruction with an OE decreased by ~43%. STAR NDSI collection completely removes clouds and accurately presents snow distribution, with an OE further decreased from ~17% to ~7%. The generation procedure in XJ has two strengths. Firstly, the satellite-borne sensors can accurately capture the snow events on the ground due to the generally thick snow averaging approximately 20 cm. Secondly, the gap-filling approach with comprehensive consideration of spatial and temporal correlation has outstanding reliability due to the significant periodicity of snow variation. It can be inferred that the NDSI datasets in NC have high accuracy because of the similar snow conditions, despite

the lack of in-situ data in this region.

By contrast, despite the satisfactory performance of OAs and CEs, the OEs of three snow cover datasets over TP are as remarkably high as 72%, 40%, and 39% even at the snow depth threshold of 1 cm (Table 5). This finding indicates the omission of a large number of snow-covered pixels. The specific reasons are as follows. Firstly, the original MODIS NDSI maps frequently underestimate the snow presence throughout the snow period because discriminating the shallow snow pixels with an averaged snow depth of approximately 4 cm over TP is challenging. Secondly, the credibility of the spatio-temporal contextual information is relatively low because the snow rapidly and irregularly varies due to the extremely complex topographic and climatic conditions, leading to a further decrease in the accuracy of the gap-filled results. Lastly, the meteorological stations over TP are unevenly distributed and are mostly located in low- and medium-altitude/latitude areas dominated by transient snow. Consequently, the evaluation results slightly exaggerate the real OEs.

Overall, STAR NDSI collection is capable of snow status estimation, eliminating cloud contamination in TAC NDSI dataset, and capturing more snow events than NIEER AVHRR SCE dataset. However, the accuracy of STAR NDSI collection has a significant regional heterogeneity. On the one hand, the accuracy over TP is lower than that of XJ and NC, which is consistent with the characteristic of the original MODIS NDSI maps. On the other hand, the permanent and periodic snow regime regions reconstructed by STAR have prominently high accuracy, while the transient snow-covered regions are easily omitted. Fortunately, the monitoring of permanent and periodic snow plays a key role in most snow-related investigations.

Table 4. Classification statistics based on in XJ.

Indicators	Snow depth > 0 cm (Snow fraction = 30%)			Snow depth > 1 cm (Snow fraction = 28%)		
	TAC	NIEER	STAR	TAC	NIEER	STAR
	OA	0.81	0.94	0.95	0.82	0.94
CE	0.02	0.02	0.04	0.02	0.03	0.05
OE	0.60	0.17	0.07	0.58	0.15	0.05

Table 5. Classification statistics over TP.

Indicators	Snow depth > 0 cm (Snow fraction = 5%)			Snow depth > 1 cm (Snow fraction = 3%)		
	TAC	NIEER	STAR	TAC	NIEER	STAR
	OA	0.94	0.93	0.95	0.96	0.94
CE	0.01	0.04	0.02	0.02	0.05	0.03
OE	0.78	0.53	0.52	0.72	0.42	0.39

Note: TAC, NIEER, and STAR represent TAC NDSI, NIEER AVHRR SCE, and STAR NDSI datasets, respectively.

3.2 Validation based on Landsat NDSI maps

...Two evaluations including a cross-comparison of TAC NDSI, MODIS CGF NDSI, and STAR NDSI datasets and an internal comparison of clear-sky and cloud-cover areas are described in detail below.

For the cross-comparison, the visual effects of three NDSI datasets on 8 January 2018 and 3 February 2018 are shown in Fig. 4. TAC NDSI dataset is still heavily obscured by clouds. Although MODIS CGF NDSI dataset completely removes clouds from the MOD10A1 product, it is difficult to accurately retrieve periodic and transient

snow cover areas due to the simplicity of the cloud-gap-filled method. Specifically, the gaps are filled by retaining clear-sky observations from previous days. However, snow patterns under cloud cover are likely to change significantly during these days. Therefore, snow cover is significantly underestimated during accumulation (Fig. 4, a2) and overestimated during ablation (Fig. 4, b2). By contrast, STAR NDSI collection preeminently captures the snow dynamics under temporally continuous clouds, attributing to the spatio-temporal adaptive fusion strategy. Furthermore, the three NDSI datasets are quantitatively assessed by Landsat NDSI maps.

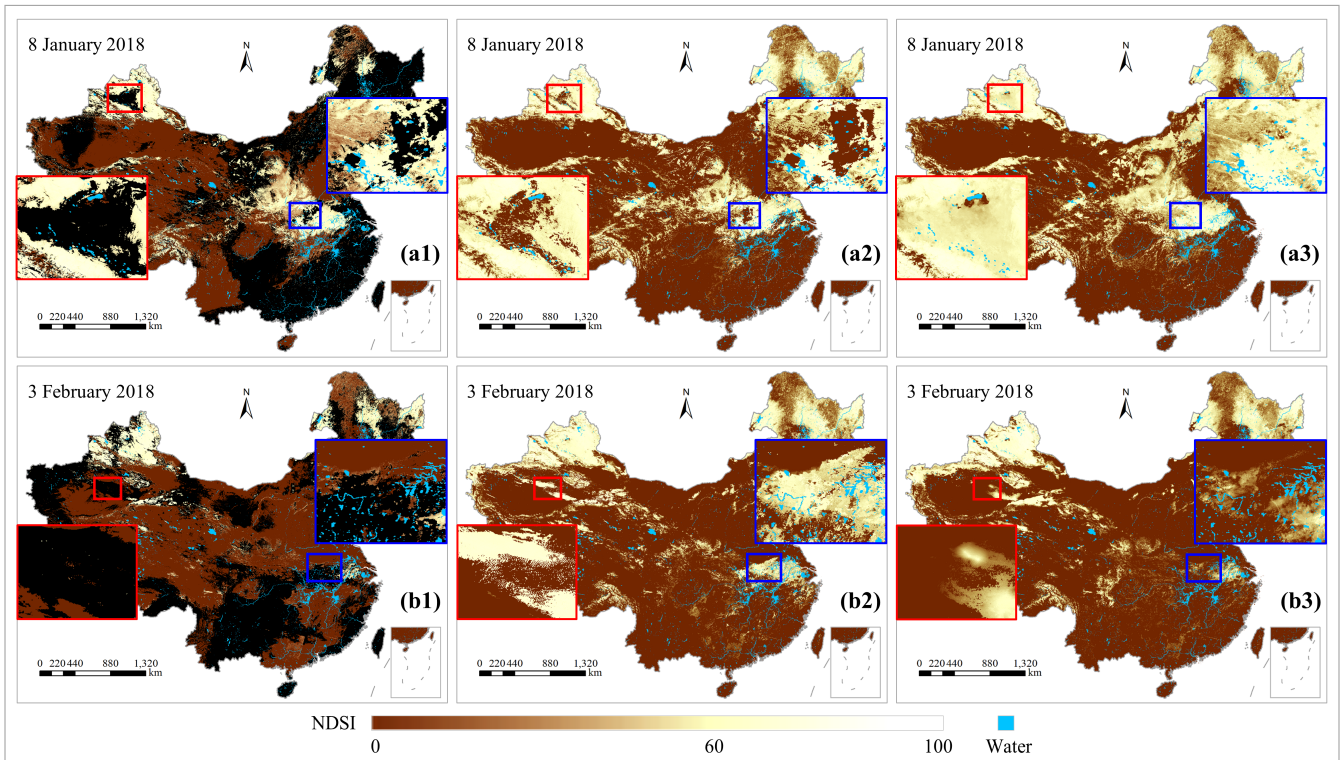


Figure 4. Comparison of TAC NDSI (column 1), MODIS CGF NDSI (column 2), and STAR NDSI (column 3) products on 8 January 2018 (group a) and 3 February 2018 (group b).

As the average cloud cover is as high as 40.7%, TAC NDSI dataset has a low correlation with Landsat NDSI maps, with an average CC of 0.46 (Table 6). The cloud-free MODIS CGF NDSI dataset enhances the correlation with Landsat NDSI maps, with an average CC of 0.73. By contrast, the spatiotemporally continuous STAR NDSI dataset are highly consistent with Landsat NDSI maps, with an average CC further increased to 0.84. Compared with TAC NDSI and MODIS CGF NDSI datasets, the average RMSE of STAR NDSI dataset is decreased by 9.06 and 5.58, respectively. The positive AEs reveal that NDSI values for snow pixels in MODIS CGF NDSI and STAR NDSI datasets are generally higher than those of Landsat NDSI maps. In terms of snow coverage, STAR NDSI dataset notably improves the detection of snow events compared to the other two datasets, with an average absolute SRD decreased by 31.1% and 2.4% (SRD indicates the difference of snow rate between MODIS and Landsat NDSI datasets). Consequently, STAR NDSI collection is a more promising snow

cover product than TAC NDSI and MODIS CGF NDSI datasets, contributing to related hydrological and meteorological studies.

Table 6. Performance statistics for two MODIS NDSI datasets against Landsat NDSI maps.

Region_Date	Cloud cover (%)	CC			RMSE			AE			SRD (%)		
		TAC	CGF	STAR	TAC	CGF	STAR	TAC	CGF	STAR	TAC	CGF	STAR
NC1_20180225	61.4	0.49	0.90	0.87	25.64	20.20	17.10	-11.59	18.35	15.07	-60.1	1.0	1.0
NC2_20180311	43.6	0.69	0.72	0.83	26.75	19.77	13.87	-9.36	15.72	12.14	-43.1	-5.7	-1.7
NC3_20180311	34.6	0.19	0.86	0.86	18.61	20.97	8.79	-10.26	10.78	0.15	-34.2	0.0	-2.8
NC4_20180318	16.3	0.73	0.95	0.98	21.50	15.03	10.25	-3.33	8.26	5.42	-16.6	0.5	-1.1
CCR1_20180203	14.9	0.20	0.93	0.95	11.53	14.91	5.04	-3.56	6.55	1.54	-11.4	4.2	2.8
CCR2_20180203	95.0	-0.07	0.52	0.73	14.26	38.77	8.43	-9.07	32.76	0.10	-47.8	29.8	-5.4
TP1_20180322	36.3	0.39	0.75	0.83	18.03	14.26	10.70	-5.30	2.02	0.77	-13.8	1.2	1.3
TP2_20180225	22.4	0.54	0.71	0.82	25.50	17.92	15.27	-9.66	-2.62	-0.30	-27.8	-11.5	-9.1
TP3_20180320	15.3	0.29	0.31	0.74	11.40	11.64	7.91	-2.89	-2.37	-1.49	-6.7	-5.9	-3.5
TP4_20180401	29.5	0.47	0.51	0.79	30.94	29.60	16.64	-16.86	-16.36	-3.71	-31.6	-29.2	-8.3
TP5_20180307	42.5	0.47	0.92	0.92	30.00	13.80	13.80	-11.76	7.67	7.67	-36.0	1.0	1.0
TP6_20180305	64.9	0.17	0.76	0.78	42.26	17.26	14.53	-32.30	-4.49	4.67	-66.1	-10.9	-2.9
TP7_20180107	60.8	0.44	0.75	0.80	28.13	18.09	18.08	-15.95	-0.48	6.04	-60.0	-19.2	-12.6
TP8_20180128	34.6	0.49	0.38	0.82	11.98	28.32	10.65	0.67	-4.91	2.68	1.1	-47.7	4.3
XJ1_20180105	52.2	0.79	0.89	0.86	27.53	22.78	22.81	-4.00	20.21	22.18	-52.2	8.4	0.1
XJ2_20180213	23.4	0.64	0.82	0.92	23.55	10.65	20.81	7.13	2.68	18.29	-14.8	4.3	7.2
XJ3_20180220	56.0	0.56	0.73	0.86	26.35	24.83	18.78	-9.87	21.24	16.06	-51.2	2.8	1.9
XJ4_20180103	23.5	0.70	0.65	0.74	28.94	25.58	28.86	15.70	22.93	26.66	-21.8	-1.1	-0.2
XJ5_20180220	46.1	0.55	0.87	0.92	23.55	15.95	11.99	-10.44	5.59	2.28	-32.7	-4.1	-8.0
Average	40.7	0.46	0.73	0.84	23.50	20.02	14.44	-7.51	7.55	7.17	-33.0	-4.3	-1.9

Note: TAC, CGF, and STAR represent TAC NDSI, MODIS CGF NDSI, and STAR NDSI datasets, respectively.

In addition to the cross-comparison of TAC NDSI, MODIS CGF NDSI, and STAR NDSI datasets, an internal comparison of STAR NDSI collection in clear-sky areas and cloud-cover areas was performed based on Landsat NDSI maps, to highlight the accuracy of the recovered pixels in STAR NDSI collection...

Q3. The lack of depth in the result analysis that makes the study inconclusive. Please emphasize the unique contributions in the present study in the comparison with the above listed cloud-free NDSI dataset and snow cover extent datasets over China.

Response: Thank you very much for the suggestion. More rigorous evaluation and more detailed analysis were added to the Results (Section 3), as shown in the response to Q2. Furthermore, we re-emphasized our contributions in the Conclusions (Section 5). The related revisions are as follows:

3 Results

As mentioned above, the generation procedure of continuous snow collection includes the pre-process TAC and the key-process STAR. The remainder clouds of 30.62% in the entire collection after TAC are completely removed by STAR. To elaborate the reliability of STAR NDSI collection, TAC NDSI, NIEER AVHRR SCE, and MODIS CGF NDSI products are used as baseline data. Specifically, based on in-situ snow depth measurements, the classification accuracy of STAR NDSI collection is compared with those of TAC NDSI and NIEER AVHRR SCE datasets. In addition, based on Landsat NDSI maps, its numerical accuracy is compared with those of TAC NDSI and MODIS CGF NDSI datasets. This section presents the evaluation results, followed by an exemplary application.

3.1 Validation against in-situ snow depth measurements

...Table 4 demonstrates that NIEER AVHRR SCE and STAR NDSI datasets preeminently capture the snow dynamics in XJ referring to the in-situ measurements, with OAs more than 90%. However, TAC NDSI dataset is insufficient to accurately describe the snow cover variability. Although CEs perform well regardless of the snow depth threshold, OEs of TAC NDSI collection are extremely high, indicating that many cloud-covered areas are dominated by snow. NIEER AVHRR SCE dataset partially retrieves snow pixel under cloud obstruction with an OE decreased by ~43%. STAR NDSI collection completely removes clouds and accurately presents snow distribution, with an OE further decreased from ~17% to ~7%. The generation procedure in XJ has two strengths. Firstly, the satellite-borne sensors can accurately capture the snow events on the ground due to the generally thick snow averaging approximately 20 cm. Secondly, the gap-filling approach with comprehensive consideration of spatial and temporal correlation has outstanding reliability due to the significant periodicity of snow variation. It can be inferred that the NDSI datasets in NC have high accuracy because of the similar snow conditions, despite the lack of in-situ data in this region.

By contrast, despite the satisfactory performance of OAs and CEs, the OEs of three snow cover datasets over TP are as remarkably high as 72%, 40%, and 39% even at the snow depth threshold of 1 cm (Table 5). This finding indicates the omission of a large number of snow-covered pixels. The specific reasons are as follows. Firstly, the original MODIS NDSI maps frequently underestimate the snow presence throughout the snow period because discriminating the shallow snow pixels with an averaged snow depth of approximately 4 cm over TP is challenging. Secondly, the credibility of the spatio-temporal contextual information is relatively low because the snow rapidly and irregularly varies due to the extremely complex topographic and climatic conditions, leading to a further decrease in the accuracy of the gap-filled results. Lastly, the meteorological stations over TP are unevenly distributed and are mostly located in low- and medium-altitude/latitude areas dominated by transient snow.

Consequently, the evaluation results slightly exaggerate the real OEs.

Overall, STAR NDSI collection is capable of snow status estimation, eliminating cloud contamination in TAC NDSI dataset, and capturing more snow events than NIEER AVHRR SCE dataset...

3.2 Validation based on Landsat NDSI maps

...Two evaluations including a cross-comparison of TAC NDSI, MODIS CGF NDSI, and STAR NDSI datasets and an internal comparison of clear-sky and cloud-cover areas are described in detail below.

For the cross-comparison, the visual effects of three NDSI datasets on 8 January 2018 and 3 February 2018 are shown in Fig. 4. TAC NDSI dataset is still heavily obscured by clouds. Although the MODIS CGF NDSI dataset completely removes clouds from the MOD10A1 product, it is difficult to accurately retrieve periodic and transient snow cover areas due to the simplicity of the cloud-gap-filled method. Specifically, the gaps are filled by retaining clear-sky observations from previous days. However, snow patterns under cloud cover are likely to change significantly during these days. Therefore, snow cover is significantly underestimated during accumulation (Fig. 4, a2) and overestimated during ablation (Fig. 4, b2). By contrast, STAR NDSI collection preeminently captures the snow dynamics under temporally continuous clouds, attributing to the spatio-temporal adaptive fusion strategy. Furthermore, the three NDSI datasets are quantitatively assessed by Landsat NDSI maps.

As the average cloud cover is as high as 40.7%, TAC NDSI dataset has a low correlation with Landsat NDSI maps, with an average CC of 0.46 (Table 6). The cloud-free MODIS CGF NDSI dataset enhances the correlation with Landsat NDSI maps, with an average CC of 0.73. By contrast, the snow dynamics presented by the spatiotemporally continuous STAR NDSI dataset are highly consistent with Landsat NDSI maps, with an average CC further increased to 0.84. Compared with TAC NDSI and MODIS CGF NDSI datasets, the average RMSE of STAR NDSI dataset is decreased by 9.06 and 5.58, respectively. The positive AEs reveal that NDSI values for snow pixels in MODIS CGF NDSI and STAR NDSI datasets are generally higher than those of Landsat NDSI maps. In terms of snow coverage, STAR NDSI dataset notably improves the detection of snow events compared to the other two datasets, with an average absolute SRD decreased by 31.1% and 2.4% (SRD indicates the difference of snow rate between MODIS and Landsat NDSI datasets). Consequently, STAR NDSI collection is a more promising snow cover product than TAC NDSI and MODIS CGF NDSI datasets, contributing to related hydrological and meteorological studies...

5 Conclusions

... (2) The cloud-free collection can accurately estimate the snow dynamics, highly consistent with in-situ snow depth and Landsat NDSI maps. Specifically, STAR NDSI collection eliminates cloud contamination and

preeminently improves the overall performance of TAC NDSI dataset. Due to the higher spatial resolution and larger dynamic range, the classification accuracy of STAR NDSI collection is higher than that of NIEER AVHRR SCE dataset. In terms of numerical accuracy, it is superior to MODIS CGF NDSI dataset, since the spatio-temporal adaptive fusion method generally outperforms the simplified MDC method. Additionally, it has a satisfactory accuracy in original cloud-cover areas...

References

- Hao, X., Huang, G., Che, T., Ji, W., Sun, X., Zhao, Q., Zhao, H., Wang, J., Li, H., and Yang, Q.: The NIEER AVHRR snow cover extent product over China – a long-term daily snow record for regional climate research, *Earth Syst. Sci. Data*, 13, 4711-4726, <https://doi.org/10.5194/essd-13-4711-2021>, 2021.
- Huang, X. D., Deng, J., Ma, X. F., Wang, Y. L., Feng, Q. S., Hao, X. H., and Liang, T. G.: Spatiotemporal dynamics of snow cover based on multi-source remote sensing data in China, *The Cryosphere*, 10, 2453-2463, <https://doi.org/10.5194/tc-10-2453-2016>, 2016.
- Jing, Y. H., Shen, H. F., Li, X. H., and Guan, X. B.: A Two-Stage Fusion Framework to Generate a Spatio-Temporally Continuous MODIS NDSI Product over the Tibetan Plateau, *Remote Sensing*, 11, 2261, <https://doi.org/10.3390/rs11192261>, 2019.
- Muhammad, S., and Thapa, A.: Daily Terra-Aqua MODIS cloud-free snow and Randolph Glacier Inventory 6.0 combined product (M*D10A1GL06) for high-mountain Asia between 2002 and 2019, *Earth Syst. Sci. Data*, 13, 767-776, <https://doi.org/10.5194/essd-13-767-2021>, 2021.
- Zhang, H., Zhang, F., Zhang, G., Che, T., Yan, W., Ye, M., and Ma, N.: Ground-based evaluation of MODIS snow cover product V6 across China: Implications for the selection of NDSI threshold, *Sci. Total Environ.*, 651, 2712-2726, <https://doi.org/10.1016/j.scitotenv.2018.10.128>, 2019.

Appendix A

All quantitative evaluation results are presented here. Due to the different spatial and temporal coverage of various existing datasets, each dataset was compared with TAC NDSI and STAR NDSI datasets separately. Specifically, based on in-situ snow depth measurements, the classification accuracy of STAR NDSI collection was compared with three SCA/FSC products (SCA also called SCE). Based on Landsat NDSI maps, the numerical accuracy of STAR NDSI collection was compared with another NDSI product.

1. NIEER AVHRR snow cover extent product over China (Hao et al., 2021).

Table A1. Classification statistics based on in XJ.

Indicators	Snow depth > 0 cm (Snow fraction = 30%)			Snow depth > 1 cm (Snow fraction = 28%)		
	TAC	NIEER	STAR	TAC	NIEER	STAR
	OA	0.81	0.94	0.95	0.82	0.94
CE	0.02	0.02	0.04	0.02	0.03	0.05
OE	0.60	0.17	0.07	0.58	0.15	0.05

Table A2. Classification statistics over TP.

Indicators	Snow depth > 0 cm (Snow fraction = 5%)			Snow depth > 1 cm (Snow fraction = 3%)		
	TAC	NIEER	STAR	TAC	NIEER	STAR
	OA	0.94	0.93	0.95	0.96	0.94
CE	0.01	0.04	0.02	0.02	0.05	0.03
OE	0.78	0.53	0.52	0.72	0.42	0.39

Note: TAC, NIEER, and STAR represent TAC NDSI, NIEER AVHRR SCE, and STAR NDSI datasets, respectively.

2. The daily MODIS 500m snow cover extent over China (Hao et al., 2020).

Table A3. Classification statistics based on in XJ.

Indicators	Snow depth > 0 cm (Snow fraction = 30%)			Snow depth > 1 cm (Snow fraction = 28%)		
	TAC	NIEER1	STAR	TAC	NIEER1	STAR
	OA	0.81	0.93	0.95	0.82	0.93
CE	0.02	0.02	0.04	0.02	0.03	0.05
OE	0.60	0.17	0.07	0.58	0.15	0.05

Table A4. Classification statistics over TP.

Indicators	Snow depth > 0 cm (Snow fraction = 5%)			Snow depth > 1 cm (Snow fraction = 3%)		
	TAC	NIEER1	STAR	TAC	NIEER1	STAR
	OA	0.94	0.96	0.95	0.96	0.97
CE	0.01	0.01	0.02	0.02	0.01	0.03
OE	0.78	0.54	0.52	0.72	0.40	0.39

Note: TAC, NIEER1, and STAR represent TAC NDSI, NIEER MODIS SCA, and STAR NDSI datasets, respectively.

3. Daily fractional snow cover dataset over High Asia from 2002 to 2018 (Qiu et al., 2017).

Table A5. Classification statistics based on in XJ.

Indicators	Snow depth > 0 cm (Snow fraction = 30%)			Snow depth > 1 cm (Snow fraction = 28%)		
	TAC	FSC	STAR	TAC	FSC	STAR
	OA	0.82	0.79	0.95	0.83	0.80
CE	0.02	0.04	0.04	0.02	0.04	0.05
OE	0.58	0.71	0.07	0.56	0.71	0.05

Table A6. Classification statistics over TP.

Indicators	Snow depth > 0 cm (Snow fraction = 5%)			Snow depth > 1 cm (Snow fraction = 3%)		
	TAC	FSC	STAR	TAC	FSC	STAR
	OA	0.94	0.91	0.95	0.96	0.92
CE	0.02	0.06	0.02	0.02	0.06	0.03
OE	0.77	0.80	0.51	0.71	0.77	0.39

Note: TAC, FSC, and STAR represent TAC NDSI, HMA MODIS FSC, and STAR NDSI datasets, respectively. FSC greater than 50% is considered snow.

4. MODIS/Terra CGF Snow Cover Daily L3 Global 500m SIN Grid, Version 61 (Hall and Riggs, 2020).

Table A7. Performance statistics for two MODIS NDSI datasets against Landsat NDSI maps.

Region_Date	Cloud cover (%)	CC			RMSE			AE			SRD (%)		
		TAC	CGF	STAR	TAC	CGF	STAR	TAC	CGF	STAR	TAC	CGF	STAR
NC1_20180225	61.4	0.49	0.90	0.87	25.64	20.20	17.10	-11.59	18.35	15.07	-60.1	1.0	1.0
NC2_20180311	43.6	0.69	0.72	0.83	26.75	19.77	13.87	-9.36	15.72	12.14	-43.1	-5.7	-1.7
NC3_20180311	34.6	0.19	0.86	0.86	18.61	20.97	8.79	-10.26	10.78	0.15	-34.2	0.0	-2.8
NC4_20180318	16.3	0.73	0.95	0.98	21.50	15.03	10.25	-3.33	8.26	5.42	-16.6	0.5	-1.1
CCR1_20180203	14.9	0.20	0.93	0.95	11.53	14.91	5.04	-3.56	6.55	1.54	-11.4	4.2	2.8
CCR2_20180203	95.0	-0.07	0.52	0.73	14.26	38.77	8.43	-9.07	32.76	0.10	-47.8	29.8	-5.4
TP1_20180322	36.3	0.39	0.75	0.83	18.03	14.26	10.70	-5.30	2.02	0.77	-13.8	1.2	1.3
TP2_20180225	22.4	0.54	0.71	0.82	25.50	17.92	15.27	-9.66	-2.62	-0.30	-27.8	-11.5	-9.1
TP3_20180320	15.3	0.29	0.31	0.74	11.40	11.64	7.91	-2.89	-2.37	-1.49	-6.7	-5.9	-3.5
TP4_20180401	29.5	0.47	0.51	0.79	30.94	29.60	16.64	-16.86	-16.36	-3.71	-31.6	-29.2	-8.3
TP5_20180307	42.5	0.47	0.92	0.92	30.00	13.80	13.80	-11.76	7.67	7.67	-36.0	1.0	1.0
TP6_20180305	64.9	0.17	0.76	0.78	42.26	17.26	14.53	-32.30	-4.49	4.67	-66.1	-10.9	-2.9
TP7_20180107	60.8	0.44	0.75	0.80	28.13	18.09	18.08	-15.95	-0.48	6.04	-60.0	-19.2	-12.6
TP8_20180128	34.6	0.49	0.38	0.82	11.98	28.32	10.65	0.67	-4.91	2.68	1.1	-47.7	4.3
XJ1_20180105	52.2	0.79	0.89	0.86	27.53	22.78	22.81	-4.00	20.21	22.18	-52.2	8.4	0.1
XJ2_20180213	23.4	0.64	0.82	0.92	23.55	10.65	20.81	7.13	2.68	18.29	-14.8	4.3	7.2
XJ3_20180220	56.0	0.56	0.73	0.86	26.35	24.83	18.78	-9.87	21.24	16.06	-51.2	2.8	1.9
XJ4_20180103	23.5	0.70	0.65	0.74	28.94	25.58	28.86	15.70	22.93	26.66	-21.8	-1.1	-0.2
XJ5_20180220	46.1	0.55	0.87	0.92	23.55	15.95	11.99	-10.44	5.59	2.28	-32.7	-4.1	-8.0
Average	40.7	0.46	0.73	0.84	23.50	20.02	14.44	-7.51	7.55	7.17	-33.0	-4.3	-1.9

Note: TAC, CGF, and STAR represent TAC NDSI, MODIS CGF NDSI, and STAR NDSI datasets, respectively.